

NASA/TM-2004-213239



# A Sensitivity Study of the Aircraft Vortex Spacing System (AVOSS) Wake Predictor Algorithm to the Resolution of Input Meteorological Profiles

*David K. Rutishauser, Patrick Butler, and Jamie Riggins  
Langley Research Center, Hampton, Virginia*

---

June 2004

## The NASA STI Program Office . . . in Profile

Since its founding, NASA has been dedicated to the advancement of aeronautics and space science. The NASA Scientific and Technical Information (STI) Program Office plays a key part in helping NASA maintain this important role.

The NASA STI Program Office is operated by Langley Research Center, the lead center for NASA's scientific and technical information. The NASA STI Program Office provides access to the NASA STI Database, the largest collection of aeronautical and space science STI in the world. The Program Office is also NASA's institutional mechanism for disseminating the results of its research and development activities. These results are published by NASA in the NASA STI Report Series, which includes the following report types:

- **TECHNICAL PUBLICATION.** Reports of completed research or a major significant phase of research that present the results of NASA programs and include extensive data or theoretical analysis. Includes compilations of significant scientific and technical data and information deemed to be of continuing reference value. NASA counterpart of peer-reviewed formal professional papers, but having less stringent limitations on manuscript length and extent of graphic presentations.
- **TECHNICAL MEMORANDUM.** Scientific and technical findings that are preliminary or of specialized interest, e.g., quick release reports, working papers, and bibliographies that contain minimal annotation. Does not contain extensive analysis.
- **CONTRACTOR REPORT.** Scientific and technical findings by NASA-sponsored contractors and grantees.

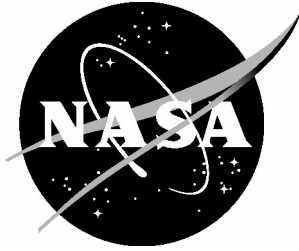
- **CONFERENCE PUBLICATION.** Collected papers from scientific and technical conferences, symposia, seminars, or other meetings sponsored or co-sponsored by NASA.
- **SPECIAL PUBLICATION.** Scientific, technical, or historical information from NASA programs, projects, and missions, often concerned with subjects having substantial public interest.
- **TECHNICAL TRANSLATION.** English-language translations of foreign scientific and technical material pertinent to NASA's mission.

Specialized services that complement the STI Program Office's diverse offerings include creating custom thesauri, building customized databases, organizing and publishing research results ... even providing videos.

For more information about the NASA STI Program Office, see the following:

- Access the NASA STI Program Home Page at <http://www.sti.nasa.gov>
- E-mail your question via the Internet to [help@sti.nasa.gov](mailto:help@sti.nasa.gov)
- Fax your question to the NASA STI Help Desk at (301) 621-0134
- Phone the NASA STI Help Desk at (301) 621-0390
- Write to:  
NASA STI Help Desk  
NASA Center for AeroSpace Information  
7121 Standard Drive  
Hanover, MD 21076-1320

NASA/TM-2004-213239



# A Sensitivity Study of the Aircraft Vortex Spacing System (AVOSS) Wake Predictor Algorithm to the Resolution of Input Meteorological Profiles

*David K. Rutishauser, Patrick Butler, and Jamie Riggins  
Langley Research Center, Hampton, Virginia*

National Aeronautics and  
Space Administration

Langley Research Center  
Hampton, Virginia 23681-2199

June 2004

Available from:

NASA Center for AeroSpace Information (CASI)  
7121 Standard Drive  
Hanover, MD 21076-1320  
(301) 621-0390

National Technical Information Service (NTIS)  
5285 Port Royal Road  
Springfield, VA 22161-2171  
(703) 605-6000

## Abstract

*The AVOSS project demonstrated the feasibility of applying aircraft wake vortex sensing and prediction technologies to safe aircraft spacing for single runway arrivals. On average, AVOSS provided spacing recommendations that were less than the current FAA prescribed spacing rules, resulting in a potential airport efficiency gain. Subsequent efforts have included quantifying the operational specifications for future Wake Vortex Advisory Systems (WakeVAS). In support of these efforts, each of the candidate subsystems for a WakeVAS must be specified. The specifications represent a consensus between the high-level requirements and the capabilities of the candidate technologies. This report documents the beginnings of an effort to quantify the capabilities of the AVOSS Prediction Algorithm (APA). Specifically, the APA horizontal position and circulation strength output sensitivity to the resolution of its wind and turbulence inputs is examined. The results of this analysis have implications for the requirements of the meteorological sensing and prediction systems comprising a WakeVAS implementation.*

## Nomenclature

B	Wingspan (m)
$b_0$	Initial wake separation ( $\pi B/4$ )
E	Eddy Dissipation Rate (EDR, $m^2/s^3$ )
$E^*$	Nondimensional Eddy Dissipation Rate
IGE	In Ground Effect
OGE	Out of Ground Effect
$y_{r,t}$	Modeled lateral position $y$ of a vortex, $t$ seconds old with a resolution $r$
$T^*$	Nondimensional time
$\Gamma$	Wake Circulation ( $m^2/s$ )
$\Gamma_0$	Initial Wake Circulation
$\Gamma^*$	Nondimensional Circulation
S	Sensitivity
$S^*$	Nondimensional Sensitivity

## Introduction

The AVOSS project [1] was successful in demonstrating the feasibility of integrating aircraft wake prediction and sensing systems to provide wake-encounter-free aircraft spacing. The spacing would be a reduction from today's static separation standards [2]. The wake sensing and prediction technologies matured through the course of the AVOSS project, but

remain in a research state of development. Future WakeVAS implementations depend on specifications for the overall system and its constituent subsystems. The specifications are derived from high-level requirements and are constrained by the capabilities of the component technologies. Efforts since the AVOSS demonstration have focused on the development of WakeVAS specifications, both through requirements development at the procedural or system users level and at the technology or systems level. This report documents the beginnings of one of the latter efforts, namely to characterize the sensitivity of the AVOSS wake Prediction Algorithm to its inputs. Details of the APA design can be found in [3]. The results and methods of this and similar future studies will be used to quantify the performance of the subsystem and to derive minimum requirements for the input data collection systems.

This report contains analysis on two of the most critical inputs for the APA. The first is a sensitivity of the wake lateral position prediction to the vertical resolution of the input crosswind profile. The second analysis is a sensitivity of the wake strength prediction to the vertical resolution of the input ambient turbulence profile.

## Crosswind Profile Sensitivity

The purpose of this study is to quantify the APA lateral wake position prediction sensitivity to the vertical resolution of its wind input. The subject of the

analysis is the AVOSS wake prediction software APA version 3.1.1 [3]. The APA uses a semi-empirical model to predict aircraft wake lateral and vertical position as well as circulation strength for the wake vortices generated by an aircraft in flight. The APA accepts as input vertical profiles of ambient winds, temperature, turbulence, and aircraft-specific initialization parameters. The wind profile is known to have a primary influence on the predicted lateral position, so only this parameter is used as the independent variable, while the other two meteorological inputs remained constant for the study.

As stated, out of ground effect (OGE, approximately 1.5 wingspans of the generating aircraft above ground) [3], the lateral position is mostly determined by the environmental winds. Descent rate, however, indirectly affects lateral position by determining how long a wake will spend at a certain altitude and be affected by that portion of the wind profile. Since descent rate changes based upon time and environmental attributes, a simplified drift model [4] can be defined as:

$$Position = \sum_{\tau=0,1\Delta\tau,2\Delta\tau,\dots}^{n\Delta\tau} v_{wind}(\tau) * \Delta T \quad (1)$$

Where  $v_{wind}$  represents an array (vertical profile) of crosswind values indexed by an altitude  $\tau$ , and  $\Delta T$  is the time in seconds the wake resides at altitude  $\tau$ .

The APA code version 3.1.1 is slightly modified to support the analysis for this study. The original code applies three interpolations to the input wind profile. The first interpolates all wind profile data to a 5 meter resolution via linear interpolation, regardless of the resolution of the input data. For the second interpolation, data values below 15 meters altitude are filled, since wind measurements start at 15 meters. The third interpolation is linear, and determines data at altitudes falling between profile points. In the modified code the first interpolation is disabled as it interferes with any resolutions that are not multiples of 5.

The source data for the analysis is the Dallas-Fort Worth (DFW) AVOSS deployment. The DFW AVOSS deployment produced the most comprehensive set of measured APA input profiles to date, and thus provides a large sample of actual wind data. This data includes ambient wind, turbulence, and temperature profiles every 30 minutes. The profiles are the output of a fusing algorithm [5] that combines data from a variety of instruments, including tower-mounted anemometers, UHF radar wind profilers, Sound

Detection and Ranging (SODAR) profilers, and Terminal Doppler Weather Radar (TDWR). The resulting wind profile data starts at 15 meters above ground level, with a resolution of 15 meters to an altitude of 60 meters above the ground, then 40 meters resolution from 60 to 100 meters in altitude, and finally 50 meters resolution from 100 meters to the top of the profile. The profile height varied between 600 and 1400 meters.

The DFW wind profiles are interpolated to obtain profiles of 1-meter resolution, used as the “truth” input to compare coarser resolutions in the analysis. A cubic spline interpolation is used for the 1-meter data since it provides an accurate fit to the measured data. The cubic spline allows for an interpolated graph that uses every original point, and has a smooth first derivative and a continuous second derivative of the interpolated data [6]. This interpolated model is then used to generate wind profiles with resolutions ranging from 1 to 250 meters. A reference resolution of zero is used to define the original data without any interpolated points. Figure 1 summarizes the data run through the APA.

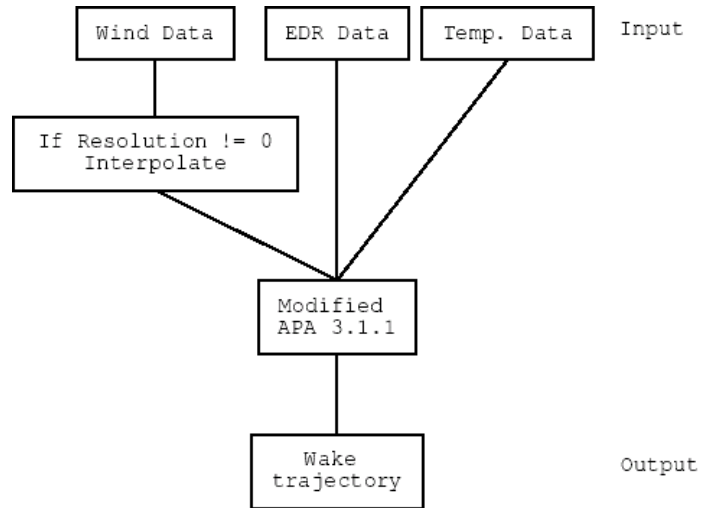


**Figure 1: Flowchart showing APA input/output data flow.**

The horizontal position error becomes large well before the 250 m resolution. In order to speed up data analysis, all further analysis is therefore limited to a maximum of 150 m resolution. It is important to perform the analysis on the full set of available data, to capture as much of the actual wind variations as possible. Roughly 2,300 30-minute weather profile observations are in the DFW data set. One “worst-case” observation is chosen to test the analysis

methods. The observation chosen is 12: 30 PM on July 20th. This observation is selected because it exhibits a

high variability in the crosswind speed. With these

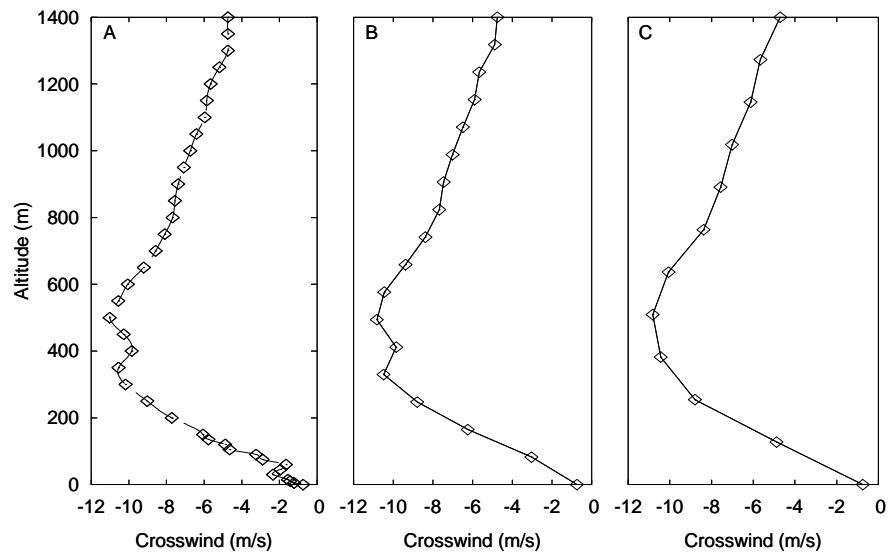


**Figure 2: A) A DFW wind profile with a cubic spline interpolated line drawn through the data. B) Decimation of profile (A) to a resolution of 80 meters. C) Decimation of profile (A) to a resolution of 120 meters.**

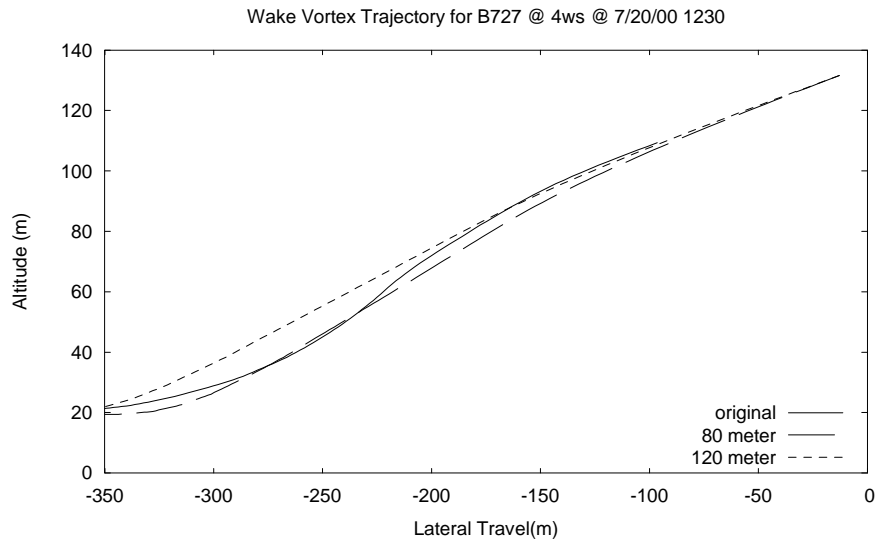


**Figure 3: A typical wake trajectory with a high-variance wind profile for decreasing degrees of resolution. Generation altitude is four B727 wingspans (ws).**

constant changes in wind speed, lowering the resolution takes out many of the kinks. This effect can be seen in Figure 2. Such errors can, over many seconds of drift, lead to hundreds of meters of position error.

Using the “worst-case” profile, a number of variables are considered. Generating aircraft altitude is varied at 2, 4, 8, and 12 wingspans of the aircraft. The types of the aircraft used are the Boeing 757, which has a 38-meter wingspan, and a Boeing 727-100 with a wingspan of 32.9 meters. The maximum gross landing weight is used for each aircraft. One goal of the analysis is to determine if the position error is aircraft dependent. Even with an aircraft-type dependence observed, it is important to note trends based on wingspan, weight, and speed of the aircraft. The position error is also measured for multiple wake ages during the trajectory, with emphasis on those where the vortex reaches a minimum altitude. The wake minimum altitudes are in ground-effect, where the vortex has a lateral velocity that is no longer solely dependent on the ambient wind profile, but is dependent on the interaction with the ground. Experimentation with the wake generation altitude resulted in the choice of 4 wingspans, which allow wakes to start out of ground effect and sink into ground effect before decaying. At 4 wingspans the vortices fall into ground effect around 96 seconds after creation. Figure 3 shows the differences in vertical and horizontal position of the predicted wake due to varying the input wind profile resolution and using the 4 wingspan initial altitude. The error at 90, 100, and 120 seconds is chosen to provide samples in and out of ground effect. Aircraft type-dependency is assessed by running the B757 and B727-100 types, using the same

initial height and times normalized to the 90, 100, and 120 seconds used for the B757, non-dimensionalized as follows:

$$T^* = T_{757} * \frac{\Gamma_0}{2\pi b_0^2} \quad (2)$$

Where  $T_{757}$  represents the raw times of 90, 100, and 120 seconds. Keeping  $T^*$  constant and solving equation (2) for the actual corresponding times for the B727 ( $T_{727}$ ) yields 95.8 seconds, 106.5 seconds, and 127.75 seconds.

Two methods for error analysis are considered: percentage error and absolute error. In finding the percentage error, the following formula is used:

$$\% Error = \frac{|y_{t,r} - y_{t,l}|}{y_{t,l}} \quad (3)$$

This follows the classic percentage error equation, using the lateral position ( $y$ ) at one meter interpolated resolution for the “truth” value. After the percentage errors are calculated for each run, the percentage errors are averaged over the entire data set. This method fails to capture the error when the winds are calm and the lateral drift is minimal, where errors as small as  $0.5b_0$  can generate over 100% error. Computing instead the absolute error with the following equation

$$Error = |y_{t,r} - y_{t,l}| \quad (4)$$

yields more consistent results. The averaged absolute errors for each aircraft type can be seen in Figures 4 and 5.

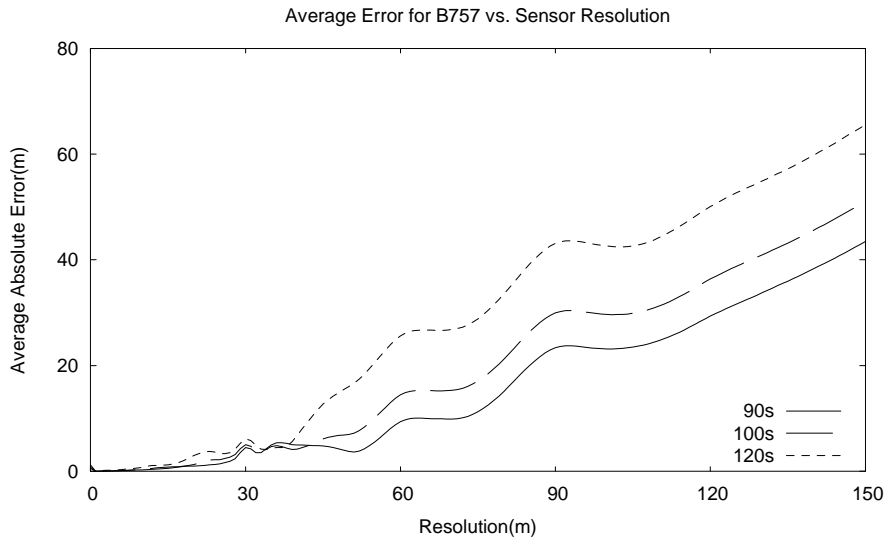


**Figure 4: Horizontal wake position error as a function of crosswind profile vertical resolution for a B757 flying at 4 wingspans altitude, 64.7 m/s velocity, plotted for three wake ages.**

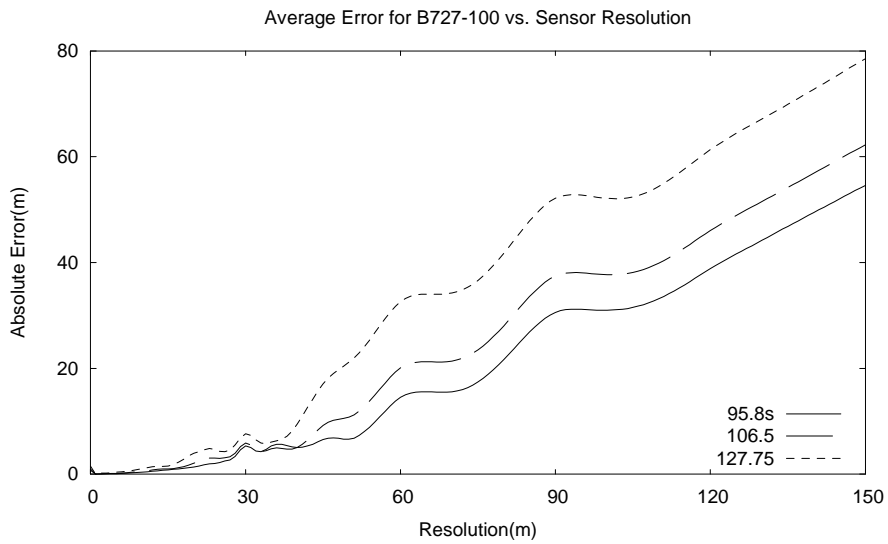


**Figure 5: Horizontal wake position error as a function of crosswind profile vertical resolution for a B727-100 flying at 4 wingspans altitude, 69.8 m/s velocity, plotted for three wake ages.**

From figures 4 and 5, the error increases slowly with decreases in resolution until around 40meters. This is due primarily to the non-uniform (and decreasing) resolution in the original DFW profiles with altitude. Clearly no observations can be made for resolutions above the resolution in the original profile. However, figures 4 and 5 indicate roughly a linear increase in position error with decreasing resolution. The slope of this error increase is dependent on the wake age. The higher sensitivity of the position error to the input resolution for the oldest wake age can be attributed to the altitudes reached by the time of this wake age. As stated previously, the input profile resolution is higher at the lower altitudes. So the potential for details in the true wind profile to be missed by sampling this profile at lower resolutions is increased. This information is useful for requirements trade analysis when applied in conjunction with wake proximity and age (strength) hazard metrics (yet to be defined with consensus). Expected position error can be estimated readily from a given input wind profile resolution capability.

Another result of interest is that an attempt to non-dimensionalize the error revealed aircraft dependencies. If aircraft effects could be normalized, the error would actually be lower on the B727 than the B757. Figures 4 and 5 show the error to be higher for the B727. The reason for this is that the B727 vortices are descending at a slower rate than the B757 vortices. Because of this slower descent rate, the vortex spends more time at a given altitude ( $\Delta T$  in Equation (1)), allowing the absolute error to build.

In order to ensure the details of real wind profiles are captured, this analysis would benefit from a re-work based on wind profiles with the highest resolutions available. A means of obtaining these profiles would be to recover the true wind profile from available lidar-measured vortex trajectories. First choosing only OGE cases, the vortex position data could be fit with a running least squares fit. Then assuming the vortex drifts with the wind and plotting vortex lateral speed ( $dy/dt$ ) with altitude would result in a vertical profile of crosswind.

## Turbulence Profile Sensitivity

The second part of this study is to evaluate APA wake strength prediction sensitivity to Eddy Dissipation Rate (EDR). EDR is a measure of the amount of turbulence in the atmosphere, and affects the circulation strength of the vortex by influencing the strength decay rate. In general, higher EDR values reduce the time to the onset of rapid decay caused by instabilities [7]

resulting in a reduced overall wake lifetime. Wake strength is output by the APA as a circulation (in  $m^2/s^2$ ) averaged over radii of 5-15 meters [8].

Typical values of EDR lie between  $10^{-5} m^2/s^3$  and  $10^{-2} m^2/s^3$ , and data taken from the DFW deployment shows that the level of EDR can range from  $10^{-7} m^2/s^3$  to  $10^0 m^2/s^3$ . EDR levels above  $10^{-2} m^2/s^3$  are atypical, and thus, are not considered. Because EDR affects the decay of vortices, it indirectly affects the wake lateral and vertical movement. A stronger pair of vortices produces a stronger mutual induction, which is the primary cause for downward movement of a vortex, and it also produces a higher self-induced lateral velocity when they reach altitudes in ground effect [9]. However, since this study focuses on the APA sensitivity to EDR, only wake circulation strength was considered as the dependent variable.

This analysis is divided into three parts. First, the maximum circulation difference for a range of EDR values is determined. Next, the time for wake vortices to decay to a particular circulation strength is examined as a function of EDR, and finally the sensitivity of wake circulation predictions to EDR is evaluated. In all experiments, a temperature profile with neutral convective stability or representing neutral stratification (constant potential temperature) was used along with a calm wind profile. This temperature profile was chosen in order to omit the effects of stratification on circulation decay rate. The EDR profiles used are constant with height.

In the first part of the study, the APA code is run for each of 19 aircraft types used for the AVOSS demonstration at DFW in the summer of 2000 [1]. Two runs are made per aircraft. One run with an input EDR value of  $10^{-7} m^2/s^3$ , and one with an input EDR value of  $10^{-2} m^2/s^3$ . For both EDR values, the vortex circulation is plotted with respect to time, yielding two curves that enclosed a range of possible circulation values for the maximum observed range of EDR inputs.

**Table 1. Maximum circulation difference Between extremes of EDR**

	Max Circulation Difference ( $m^2/s$ )	
	OGE	IGE
Large (B727)	195.295	236.621
B757	223.84	266.27
Heavy (B747)	394.704	455.335

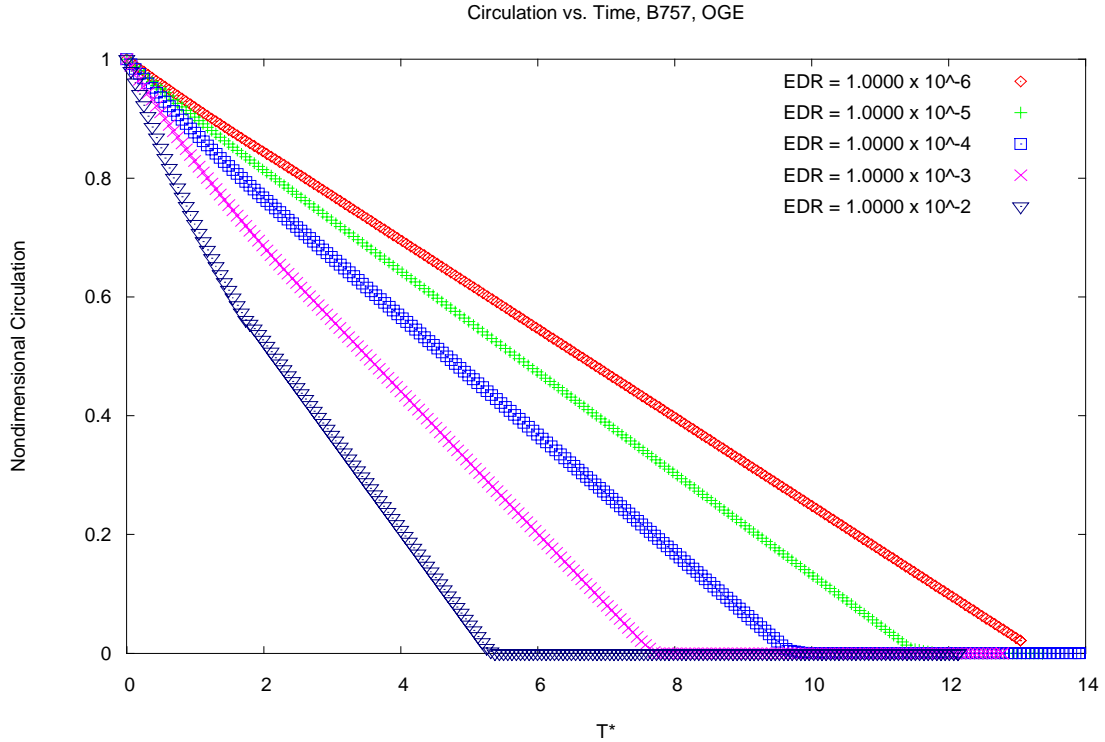


**Figure 7. APA Predicted circulation of a B757 vortex for 5 different EDR input profiles; OGE initial height.**

From this, the maximum circulation difference is extracted for each weight category at each initial height shown in Table 1. Out of ground effect (OGE) indicates that the initial aircraft height was three times its wingspan, while in ground effect (IGE) means that that initial aircraft height was one-and-a-half times its wingspan. Note that depending on the input turbulence level the OGE wakes may reach IGE heights before terminating.

Figure 7 shows the differences in decay rate for a range of EDR values. In Figure 7, the circulation is normalized by its initial value, and the time is normalized as follows:

$$T^* = T \frac{\Gamma_0}{2\pi b_0^2} \quad (5)$$

The maximum difference in vortex circulation strength for an aircraft is useful to know because it establishes the bounds of the effects of the EDR input on the APA output. The effect of the wake on a trailing aircraft

depends on its strength, the geometry of the encounter, and the size and capabilities of the trailing aircraft. If the circulation strength of a leading aircraft's wake at a particular time is known, then it is also known that for any EDR level at that same time, the circulation cannot be greater than that circulation strength plus the maximum circulation difference. Similarly, the rightmost curve in Figure 7 could be used as a worst-case bound for the circulation as a function of time that is independent of EDR.

The second part of the study examines a specific circulation rather than a range of circulation values. For each of the 19 aircraft, the APA code is run for a range of EDR values that begins at  $10^{-7} \text{ m}^2/\text{s}^3$  and ends at  $10^{-2} \text{ m}^2/\text{s}^3$ . Each APA code run corresponds to a different EDR value. In each run, the time at which vortex circulation reaches  $70 \text{ m/s}^2$  is extracted and added to a plot in which EDR is the independent variable. The  $70 \text{ m/s}^2$  threshold is the AVOSS threshold that corresponds to background turbulence.

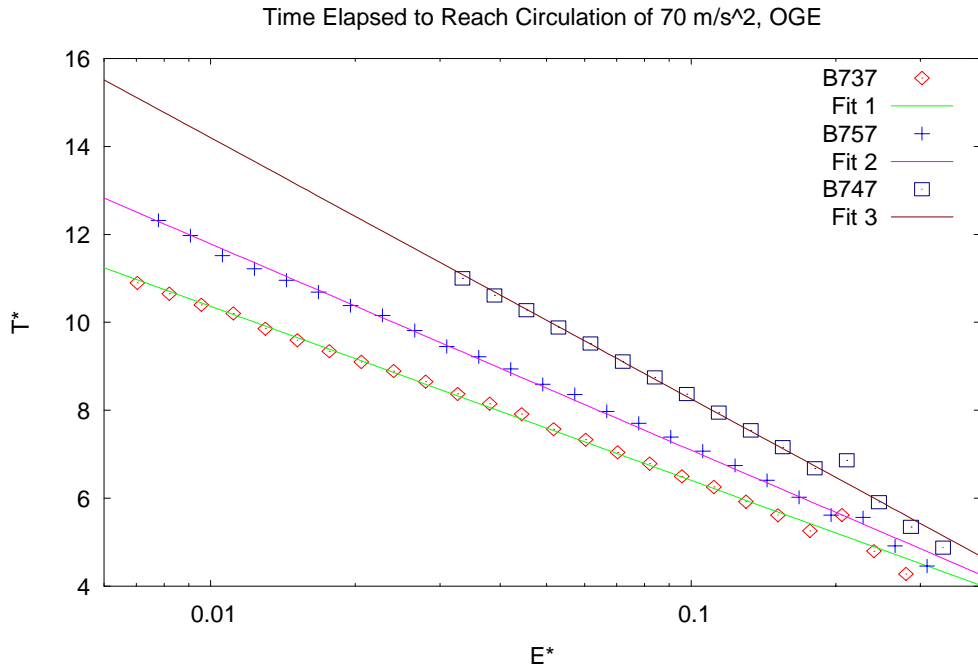


Figure 8a. Time elapsed for the vortices of three different weight category aircraft to reach a circulation threshold of  $70 \text{ m/s}^2$ , out of ground effect.

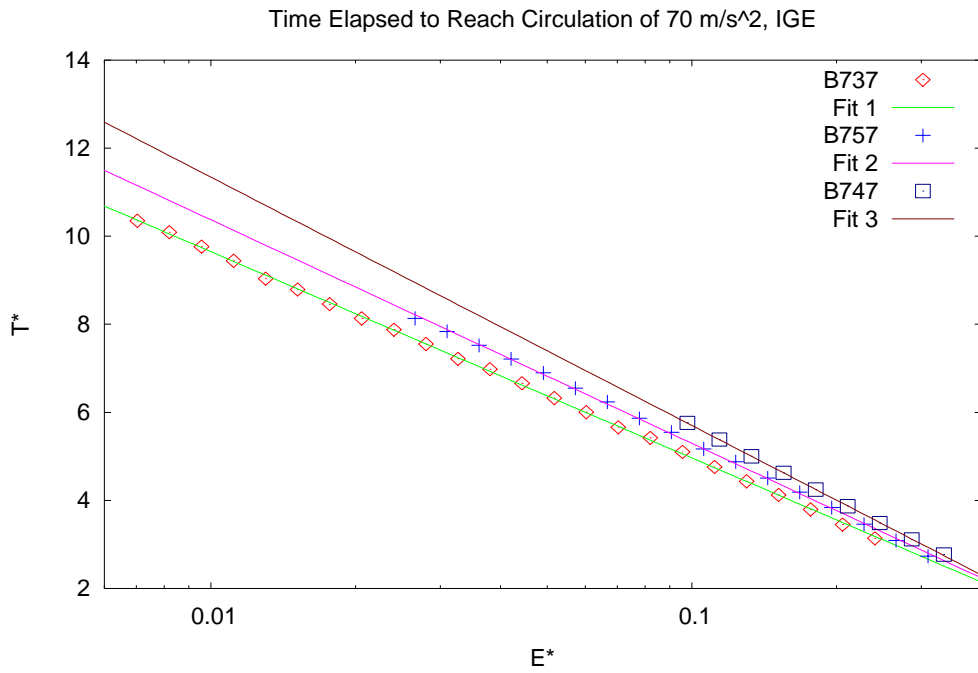


Figure 8b. Time elapsed for the vortices of three different weight category aircraft to reach a circulation threshold of  $70 \text{ m/s}^2$ , in ground effect

A candidate aircraft-independent wake strength hazard definition is a circulation that is indistinguishable from background turbulence. To compare the plots between different aircraft, the units of EDR were non-dimensionalized by the aircraft parameters as follows:

$$E^* = \frac{(Eb_0)^{1/3}}{V_0} \quad (6)$$

One plot for each FAA weight category (except small) is shown in Figure 8a for generation heights out of ground effect. Figure 8b is the same plots for wake generation in ground effect. Non-dimensionalizing by aircraft parameters shows an aircraft type dependency, which decreases with increasing values of turbulence. The IGE model is also less sensitive to these aircraft type dependences. Figure 8b also shows the limitations of APA 3.1.1 with regards to the IGE decay model being overly sensitive to the EDR. Recent studies [10] have shown the circulation decay is independent of EDR once the vortices have reached their minimum altitude IGE. Future sensitivity studies will use the latest real-time wake models such as APA 3.2 [3] that more correctly capture the IGE behavior.

In the OGE plot 8a, the logarithmic pattern changes toward the end of the trajectory. This is because the OGE algorithm is non-linear in the way it treats the

EDR effects on the circulation. In the algorithm, the normalized time at which the onset of rapid decay (Crow instability) occurs is calculated differently depending on the EDR [3].

Plots like those of Figures 8a and 8b could be used as wake decay lookup tables for a WakeVAS implementation. Measurements and predictions of EDR can be indexed to expected wake demise for the appropriate aircraft type. The same information can also be used to bound wake decay behavior for the purposes of a WakeVAS benefits analysis. For either of these purposes continued validation of the model results with observed data must occur. Figures 9a and 9b show similar plots to 8a and 8b, for a single aircraft (B757) type and three circulation thresholds. These plots serve as an example of the impact of a variable wake strength hazard metric. Instead of using a threshold of 70 m/s<sup>2</sup>, the thresholds are normalized to the wake initial strength and chosen to be 10%, 20%, and 50% of this initial value. Assuming that a wake strength hazard metric that accounts for the trailing aircraft type can be used, plots such as in figures 9a and 9b can be used to compare demise times for various choices of these thresholds. Coupled with a benefits analysis, a benefits case could be made for the inclusion of a dynamic strength hazard threshold in future WakeVAS implementations.

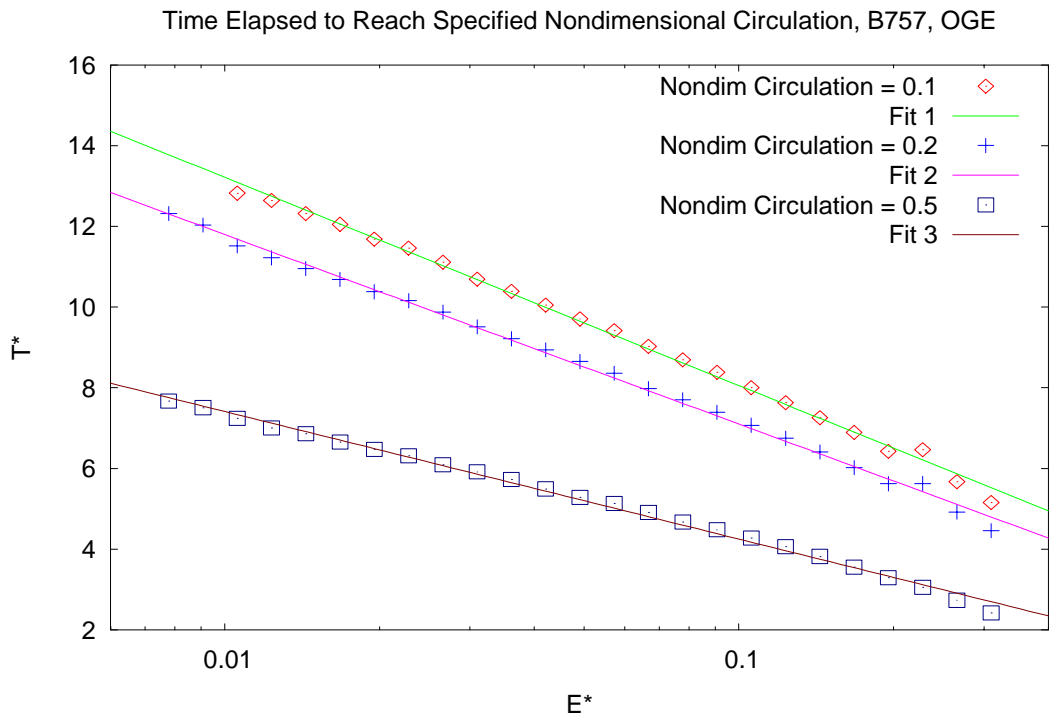


**Figure 9a.** Time elapsed for the vortices of a B757 to reach three different percentages of initial circulation strength: 10%, 20%, and 50%, generated out of ground effect

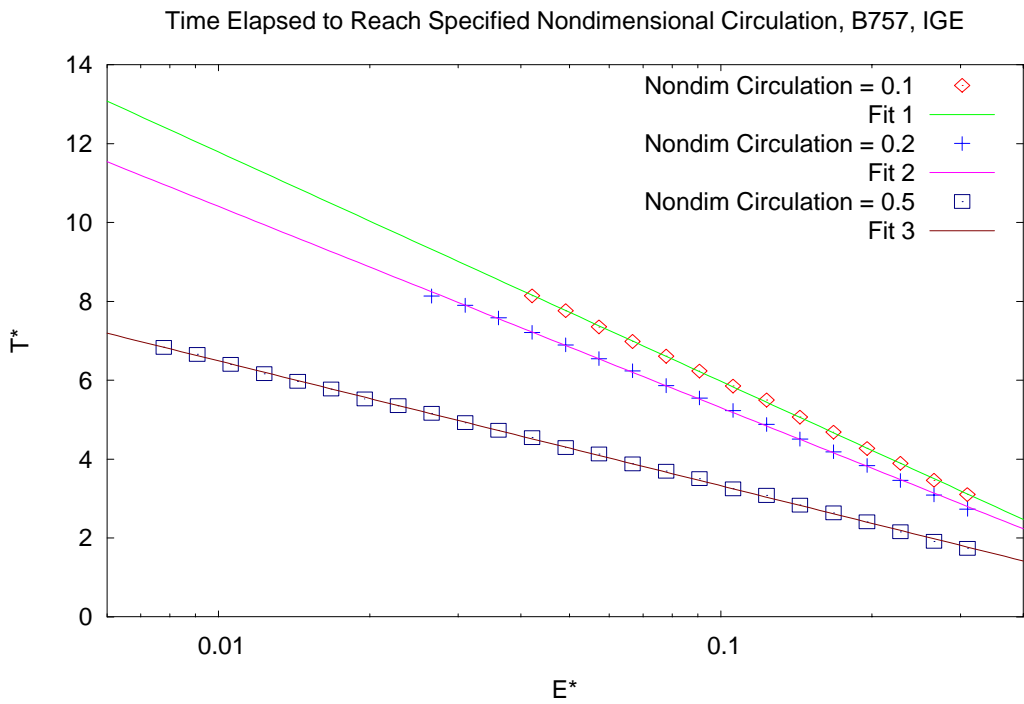


**Figure 9b.** Time elapsed for the vortices of a B757 to reach three different percentages of initial circulation strength: 10%, 20%, and 50%, generated in ground effect

Fitting an equation to the plots could provide an analytic tool for trade analysis. For example, the equation for the B757 to reach 0.2 of its initial circulation strength at out of ground effect was  $T^*(E^*) = 2.4055 - 2.03913 \cdot \log(E^*)$ . The plots for each aircraft were fairly similar. When the constants were averaged, the equation for any aircraft to reach 0.2 of its initial circulation strength at out of ground effect was  $T^*(E^*) = 2.3109 - 2.0719 \cdot \log(E^*)$ .

In the final part of the study, the sensitivity of the APA decay model to its EDR input is quantified. The classical sensitivity equation is used, which describes sensitivity as a percent change in one parameter divided by the percent change in another parameter. From this equation, the sensitivity used in this project is defined as the percent change in circulation divided by the percent change in EDR:

$$S = \frac{(\Gamma - \Gamma_p) / \Gamma}{(E - E_p) / E} \quad (7)$$

In Equation 7,  $E$  is the original EDR value,  $E_p$  is the original EDR changed by a small percentage, and  $\Gamma$  and  $\Gamma_p$  are the circulation strengths that correspond to those EDR values at a particular time, respectively.

For this project the original parameter values are perturbed by five percent.

For each of the 19 aircraft, the APA code is run for a range of EDR values that again starts at  $10^{-7} \text{ m}^2/\text{s}^3$  and ends at  $10^{-2} \text{ m}^2/\text{s}^3$ . After each run, the circulation at a particular wake age is extracted. Then the input EDR is modified by 5%, the APA code is run again, and the new circulation at the same wake age extracted. The sensitivity values are then plotted as a function of EDR. To evaluate what happens to the sensitivity at different wake ages, several of these plots are made with each corresponding to a different time. The times chosen are 15, 30, 45, and 60 seconds from generation for the B757, and are plotted in Figure 10. These times cover wake behavior both in and out of ground effect. As shown in figure 10, the sensitivity of the circulation to  $E^*$  remains relatively constant and 10% or less in magnitude over several orders of magnitude of  $E^*$ . An implication of this observation is that a WakeVAS system may operate with a low resolution requirement on its turbulence data collection system, assuming the high-level wake strength prediction requirements can still be met.

As before, the variables plotted in figure 10 are non-dimensionalized so they can be compared among different aircraft. The non-dimensionalized equations

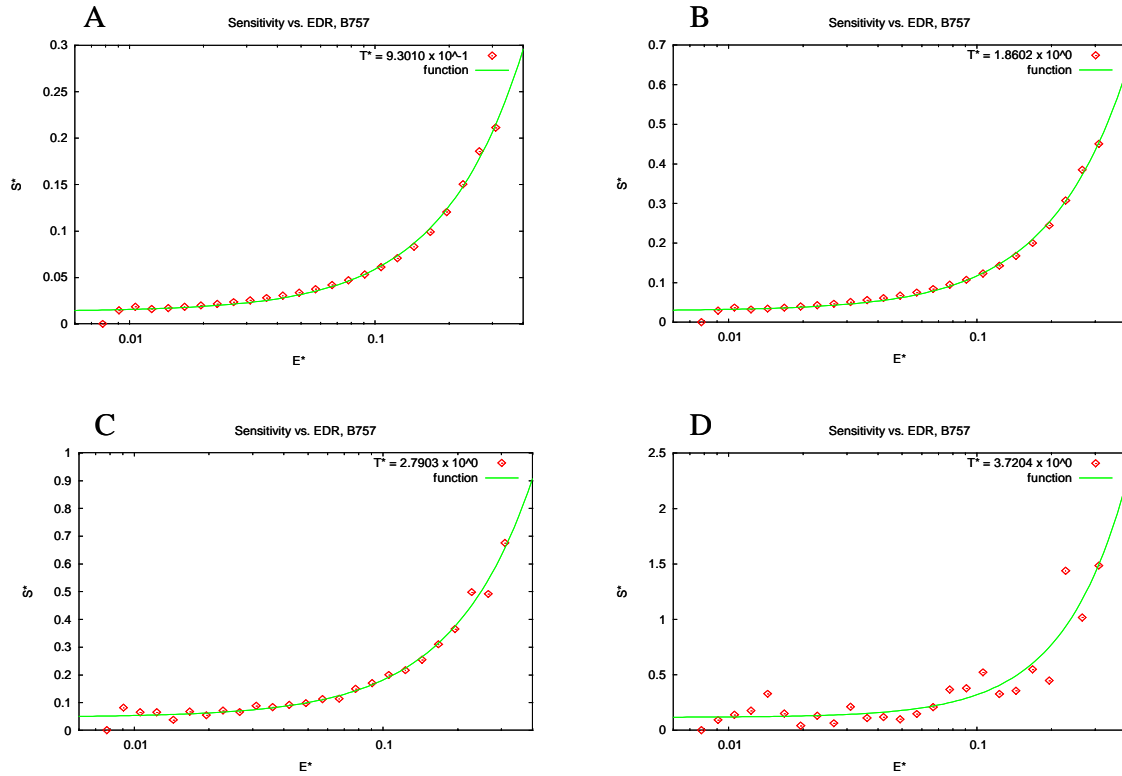


**Figure 10: Non-dimensionalized sensitivity of a B757 wake circulation strength to input non-dimensional EDR at A) 15 seconds, B) 30 seconds, C) 45 seconds, and D) 60 seconds.**

for circulation and EDR were used to define the non-dimensionalized sensitivity as follows:

$$\begin{aligned}
 S^* &= \frac{(\Gamma^* - \Gamma_p^*) / \Gamma^*}{(E^* - E_p^*) / E^*} = \\
 &= \frac{(\Gamma / \Gamma_l - \Gamma_p / \Gamma_l) / \Gamma / \Gamma_l}{((Eb_o)^{1/3} / V_o - (E_p b_o)^{1/3} / V_o) / (Eb_o)^{1/3} / V_o} = \\
 &= \frac{(\Gamma - \Gamma_p) / \Gamma}{(E^{1/3} - E_p^{1/3}) / E^{1/3}}
 \end{aligned}
 \tag{8}$$

Also shown in Figure 10, a function was fit to each sensitivity plot. Functions were compared between different aircraft, and functions were also compared between different times for the same aircraft. For instance, the equation for the B757 at 15 seconds was  $S^* = 0.940379E^{*1.31446} + 0.0132901$ . Using the B757 timeframe as a base, the nondimensional time

that corresponded to 15 seconds for a B757 was calculated, and from that the corresponding times for each aircraft are determined. An examination of the sensitivity data for the other aircraft types reveals only a weak dependency on aircraft type. Therefore, averaging the constants in the equation fits for all the aircraft types yields the equation for any aircraft at  $T^*$  corresponding to 15 seconds for the B757 is:

$$S^* = 0.8597(\varepsilon^*)^{1.2529} + 0.0118 \tag{9}$$

The weak aircraft type dependency on the sensitivity relationships is consistent for other wake ages. The data fit in equation (9) could be a useful analytic tool for requirements analysis.

A stronger dependency to wake age for the sensitivity relations is observed and shown in Figure 11. Particularly, the first constant in the equation grows larger with increasing time, while the other constants did not vary significantly.

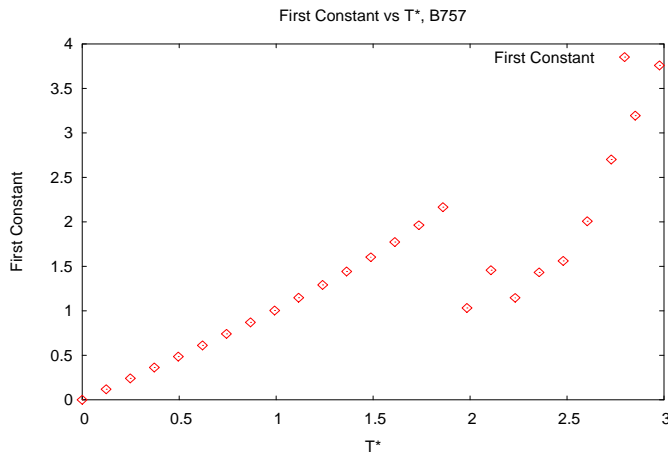


**Figure 11. B757 sensitivity equation's first constant as a function of time**

The linear pattern seen in figure 11 ends just before the plot reaches a  $T^*$  value of two. The reason for the abrupt change is the APA analytic model changes with proximity of the wake to the ground [3]. This abrupt change in pattern can also be seen in the four sensitivity plots of figure 10. In plots 10a and 10b, which are both plotted before the wake reaches a nondimensional time of 2, each data point is on or very close to the equation that mapped to the data. Conversely, in plot 10c, the nondimensional time is 2.8, and some of the data points begin to break away from the pattern. This may limit the usefulness of equation (9) to out of ground effect analysis.

## Conclusion

This report documents two analyses on the performance of a candidate subsystem for future WakeVAS implementations. The sensitivity of the APA wake lateral position and strength outputs to its corresponding inputs of crosswinds and EDR profiles was examined and quantified. From this first attempt at such an analysis, observations and analytic relations were derived that could be useful in examining subsystem performance/complexity tradeoffs during the course of WakeVAS development. For example, relationships between the crosswind profile resolution and the APA lateral wake position prediction were observed. Aircraft-independent equations for the sensitivity of the APA wake strength output to the turbulence input are also derived. It is clear from these analyses that the relationships examined are different for wakes in and out of ground effect, and can change with wake age.

During the course of WakeVAS requirements and specifications definition, similar analysis will continue to characterize the complex relationships between candidate WakeVAS subsystem performance and overall system performance. In order to arrive at

sound system specifications, an ongoing process of quantifying the capabilities of the technology and reconciling these capabilities with the overall requirements will be performed. This process will be supported by engineering studies such as those presented in this report.

## Acknowledgments

The authors wish to thank David Hamilton and Dr. Fred Proctor in the Airborne Systems Competency at NASA Langley Research Center who provided a review and many ideas and guidance for this work. Patrick Butler and Jamie Riggins performed this work under the NASA Langley Aerospace Research Summer Scholars (LARSS) program.

## References

- <sup>1</sup> O'Connor, C., Rutishauser, D.; *Enhanced Airport Capacity Through Safe, Dynamic Reductions in Aircraft Separation: NASA's Aircraft VORTEX Spacing System (AVOSS)*, Journal of Air Traffic Control, Volume 43, No. 3, October-December 2001, p. 4-10.
- <sup>2</sup> *Air Traffic Controller's Handbook*, FAA Order# 7110.65N, February 2004.
- <sup>3</sup> Robins, R., Delisi, D.; *NWRA AVOSS Wake Vortex Prediction Algorithm Version 3.1.1*, NASA/CR-2002-211746, June 2002.
- <sup>4</sup> Hamilton, D., W., Proctor, F., H; *Wake Vortex Transport in Proximity to the Ground*, 19<sup>th</sup> Digital Avionics Systems Conference, October 7-13, 2000.
- <sup>5</sup> Cole, R., Denneno, A., Matthews, M.; *The AVOSS Winds Analysis System*, Project Report NASA/L-5, Lincoln Laboratory, Massachusetts Institute of Technology, April, 2001.
- <sup>6</sup> Press, Willaim H. et al. *Numerical Recipes in C: The art of Scientific Computing*. 2<sup>nd</sup> ed. New York, NY: Cambridge University Press, 2002.
- <sup>7</sup> Sarpkaya, T.; *New Model for Vortex Decay in the Atmosphere*, AIAA 99-0761, 37th AIAA Aerospace Sciences Meeting & Exhibit, January 11-14, 1999, Reno, NV, also published Journal of Aircraft, 2000, Vol. 37, No. 1, pgs. 53-61.
- <sup>8</sup> Hinton, D., A., Tatnall, C. R.; *A Candidate Wake Vortex Strength Definition for Application to the NASA Aircraft Vortex Spacing System (AVOSS)*, NASA Technical Memorandum 110343, September 1997.
- <sup>9</sup> F.H. Proctor, D.A. Hinton, J. Han, D.G. Schowalter and Y.-L. Lin, *Two Dimensional Wake Vortex Simulations in the Atmosphere: Preliminary Sensitivity Studies*, 35th AIAA Aerospace Sciences Meeting and Exhibit, Reno, Nevada, AIAA 97-0056, January 6-9, 1997, pp. 13

---

<sup>10</sup> Proctor, F., H., Hamilton, D., W., Han, J.; *Wake Vortex Transport and Decay in Ground Effect: Vortex Linking with the Ground*, AIAA-2000-0757, 38<sup>th</sup> Aerospace Sciences Meeting & Exhibit, January 10-13, 2000, Reno, NV.

**REPORT DOCUMENTATION PAGE**

*Form Approved  
OMB No. 0704-0188*

The public reporting burden for this collection of information is estimated to average 1 hour per response, including the time for reviewing instructions, searching existing data sources, gathering and maintaining the data needed, and completing and reviewing the collection of information. Send comments regarding this burden estimate or any other aspect of this collection of information, including suggestions for reducing this burden, to Department of Defense, Washington Headquarters Services, Directorate for Information Operations and Reports (0704-0188), 1215 Jefferson Davis Highway, Suite 1204, Arlington, VA 22202-4302. Respondents should be aware that notwithstanding any other provision of law, no person shall be subject to any penalty for failing to comply with a collection of information if it does not display a currently valid OMB control number.  
**PLEASE DO NOT RETURN YOUR FORM TO THE ABOVE ADDRESS.**

<b>1. REPORT DATE (DD-MM-YYYY)</b> 01-06-2004		<b>2. REPORT TYPE</b> Technical Memorandum		<b>3. DATES COVERED (From - To)</b>	
<b>4. TITLE AND SUBTITLE</b> A Sensitivity Study of the Aircraft Vortex Spacing System (AVOSS) Wake Predictor Algorithm to the Resolution of Input Meteorological Profiles				<b>5a. CONTRACT NUMBER</b>	
				<b>5b. GRANT NUMBER</b>	
				<b>5c. PROGRAM ELEMENT NUMBER</b>	
<b>6. AUTHOR(S)</b> Rutishauser, David K.; Butler, Patrick; and Riggins, Jamie				<b>5d. PROJECT NUMBER</b>	
				<b>5e. TASK NUMBER</b>	
				<b>5f. WORK UNIT NUMBER</b> 23-727-04	
<b>7. PERFORMING ORGANIZATION NAME(S) AND ADDRESS(ES)</b> NASA Langley Research Center Hampton, VA 23681-2199				<b>8. PERFORMING ORGANIZATION REPORT NUMBER</b>  L-18383	
<b>9. SPONSORING/MONITORING AGENCY NAME(S) AND ADDRESS(ES)</b> National Aeronautics and Space Administration Washington, DC 20546-0001				<b>10. SPONSOR/MONITOR'S ACRONYM(S)</b>  NASA	
				<b>11. SPONSOR/MONITOR'S REPORT NUMBER(S)</b>  NASA/TM-2004-213239	
<b>12. DISTRIBUTION/AVAILABILITY STATEMENT</b> Unclassified - Unlimited Subject Category 03 Availability: NASA CASI (301) 621-0390      Distribution: Nonstandard					
<b>13. SUPPLEMENTARY NOTES</b> An electronic version can be found at <a href="http://techreports.larc.nasa.gov/ltrs/">http://techreports.larc.nasa.gov/ltrs/</a> or <a href="http://ntrs.nasa.gov">http://ntrs.nasa.gov</a> Butler and Riggins performed this work under the NASA Langley Aerospace Research Summer Scholars (LARSS) Program.					
<b>14. ABSTRACT</b> The AVOSS project demonstrated the feasibility of applying aircraft wake vortex sensing and prediction technologies to safe aircraft spacing for single runway arrivals. On average, AVOSS provided spacing recommendations that were less than the current FAA prescribed spacing rules, resulting in a potential airport efficiency gain. Subsequent efforts have included quantifying the operational specifications for future Wake Vortex Advisory Systems (WakeVAS). In support of these efforts, each of the candidate subsystems for a WakeVAS must be specified. The specifications represent a consensus between the high-level requirements and the capabilities of the candidate technologies. This report documents the beginnings of an effort to quantify the capabilities of the AVOSS Prediction Algorithm (APA). Specifically, the APA horizontal position and circulation strength output sensitivity to the resolution of its wind and turbulence inputs is examined. The results of this analysis have implications for the requirements of the meteorological sensing and prediction systems comprising a WakeVAS implementation.					
<b>15. SUBJECT TERMS</b> Aircraft spacing; Aircraft wake vortex					
<b>16. SECURITY CLASSIFICATION OF:</b>			<b>17. LIMITATION OF ABSTRACT</b>	<b>18. NUMBER OF PAGES</b>	<b>19a. NAME OF RESPONSIBLE PERSON</b>
<b>a. REPORT</b>	<b>b. ABSTRACT</b>	<b>c. THIS PAGE</b>			STI Help Desk (email: <a href="mailto:help@sti.nasa.gov">help@sti.nasa.gov</a> )
U	U	U	UU	19	<b>19b. TELEPHONE NUMBER (Include area code)</b> (301) 621-0390